European Review for Medical and Pharmacological Sciences 2024; 28: 778-788

Biological differences and molecular mechanism of different peripheral nerves after injury

W.-L. GONG[1], Y.-N. ZHANG[1], J. ZHANG[2], X. JIANG[2], W.-J. XIAN[3]

[1]School of Clinical Medicine, Weifang Medical University, Weifang, China
[2]Department of Orthopedic Surgery, Weifang People's Hospital, China
[3]Department of Hepatobiliary Surgery, Weifang People's Hospital, Shandong, China

Abstract. – OBJECTIVE: The aim of the study was to analyze the apoptosis of neurons and the differences in expression of Bcl-2 and Bax protein in the neurons in the corresponding spinal cord segment after the repair of the tibial nerve (TN) and common peroneal nerve (CPN) in rats.

MATERIALS AND METHODS: 126 healthy male Sprague-Dawley (SD) rats aged 7-8 weeks were randomly divided into group A (control group), group B (TN was cut and sutured), and group C (CPN was cut and sutured), with 42 rats in each group. The spinal cord tissues of rats in different groups were stained with hematoxylin-eosin (HE) on the 1st, 3rd, 7th, 14th, 21st, and 28th day after surgery; the number of neurons in anterior horn of spinal cord, axon density (AD), axon passage rate (APR), and recovery rate (RR) of muscle cell cross-sectional area (MCCA) were calculated; and differences in the expression of Bcl-2 and Bax proteins in the three groups of rats were analyzed by immunohistochemistry.

RESULTS: The results showed that there was no statistically significant difference in the muscle wet weight (MWW) RR of the three groups of rats on the 14th day after the surgery ($p>0.05$), and the MWW RRs of rats in groups B and C were higher at the 28th day after surgery in contrast to group A ($p<0.05$). The number of motor neurons in the anterior horn of spinal cord in group B was higher than that in group C at the 3rd, 7th, 14th, and 21st day after surgery ($p<0.05$); the MWW RR, MCCA, and CSARR of rats in group B were lower than those in group C ($p<0.05$); the proximal AD, distal AD, and APR in group B were higher than those of group C on the 14th and 28th day after the surgery ($p<0.05$); and there were no positive staining results in the spinal cord tissue of rats in group A after staining. The expressions of Bcl-2 and Bax in group B were higher observably than the expressions in group C ($p<0.05$), which indicated that the recovery ability of TN was stronger than that of the CPN; the expression of Bcl-2 and Bax in TN was notably higher than that of the CPN.

CONCLUSIONS: The expression of Bcl-2 and Bax was related to cell apoptosis and nerve regeneration after nerve injury. It provided a reference basis for clinical diagnosis and treatment of peripheral nerves.

Key Words:
Tibia nerve, Common peroneal nerve, Neurons, Bcl-2 protein, Bax protein, Nerve regeneration

Introduction

Peripheral nerve injury is a disease in which symptoms such as sensory disturbance, nutritional imbalance, and motor obstruction occur in nerve areas other than the central nerve caused by a variety of factors[1]. With the development of the modern economy, the number of patients with peripheral nerve injury has considerably increased. The number of patients with peripheral nerve injury accounts for about 3% of new cases in the world. Once the peripheral nerve is injured, patients will suffer from various degrees of dysfunction and even disability or death. Although the peripheral nervous system has a strong regenerative ability, only 10-25% of the function can be restored to normal, and there are still many factors that affect the repair effect after peripheral nerve injury[2]. The current research results show that the type of nerve injury, the age of the patient, and the choice of intervention time have various degrees of influence on the repair of peripheral nerves after injury[3]. Although there is a lot of research on the repair mechanism after peripheral nerve injury, it is not clear whether there is a difference between the degree and recovery ability of corresponding neuron death after different peripheral nerve injuries.

TN and CPN in the sciatic nerve are two important nerves, and the incidence in these two nerves has continued to increase in recent

Corresponding Author: Jian Zhang, MD; e-mail: rmyyzhangjian@wfmc.edu.cn

years[4]. At present, most of the research on the repair of peripheral nerve injury takes rodents as the model for study, and nerve tension-free suture is the standard method to repair the nerve injury[5]. Nerve injury causes the loss of some neurons, results in impaired nerve function, and is related to neuronal apoptosis[6]. The Bcl-2 gene is involved in the regulation of cellular anti-oxidation, apoptosis, and calcium ion channels on the cell membrane; the protein function encoded by the Bax gene is antagonistic to Bcl-2, and its expression is extremely positively correlated with cell apoptosis[7]. Current studies have shown that Bcl-2 and Bax proteins are related to neuronal cell death after nerve injury[8].

In summary, it is currently unclear whether there is a difference in the death degree and recovery ability of the corresponding neurons after different peripheral nerve injuries. Moreover, there are few studies on the expression of Bcl-2 and Bax protein after different nerve injuries. In this study, 126 healthy male SD rats aged 7-8 weeks were randomly divided into three groups for analysis and comparison, and different peripheral nerve injury models were established. In addition, biological differences after different peripheral nerve injuries and the differences in the expression of Bcl-2 and Bax proteins were analyzed so as to provide a reference for clinical diagnosis and treatment of peripheral nerve injury.

Materials and Methods

Experimental Animals and Grouping

126 healthy male SD rats aged 7-8 weeks, weighing 265-305 g were selected. 5 rats were housed in each cage in a specified pathogen-free (SPF) room for experimental animals. Conditions of the room were defined as below: room temperature of 25°C, relative humidity of about 55%, 12 hours of lighting, and free drinking and dieting. The rats were fed adaptively for two weeks. All rats were randomly divided into three groups: group A was the control group, group B was the suture group after tibial nerve transection, and group C was the suture group after common peroneal nerve transection, with 42 rats in each group.

Preparation of Peripheral Nerve Injury Model

2.5% sodium pentobarbital was used for abdominal injection anesthesia at a dose of 30 mg/kg. After the anesthesia was satisfied, all rats were fixed on the operating table in a supine position and performed with routine disinfection. Under aseptic conditions, the rats were cut with a transverse incision above the right hip to separate the muscles, exposing the right sciatic nerves bluntly. Rats in group A were not treated specially. TNs of rats in group B were bluntly separated along with the adventitia tissue, and CPNs of rats in group C were bluntly separated along with the adventitia tissue so that both groups of rats suffered from complete severance injury. Then, the rats in groups B and C were sutured with TN and CPN under a microscope with 9-0 non-invasive sutures and placed in a cage after they were awake[9]. After surgery, each rat was injected with penicillin (Shanghai Xian Feng Pharmaceutical Co., Ltd, Shanghai, China) 200,000 U in the left hip muscle every day for 3 consecutive days to prevent intraoperative and postoperative infection. Iodophor was disinfected at the area of the incision once a day after surgery. The rats were allowed to move freely in the cage. During the first three days after the surgery, the diet and activities of the rats were observed daily to check if there were any abnormalities, and the healing of the incision was observed at any time. All rats survived after surgery. In rats, the foot ptosis and plantar-flexion movement were lost, and the gastrocnemius muscle of the lower limbs on the surgical side was gradually atrophied, with the loss of the full appearance, which became more and more evident compared with the opposite side. Besides, no foot ulceration or autotomy was found in all rats.

Morphological Observation and Counting Method of Motor Neurons in the Anterior Horn of the Spinal Cord

The rats in groups A, B, and C were divided into the 1st, 3rd, 7th, 14th, 21st, and 28th groups, with 7 rats in each group. After the survival time of the successfully prepared model rats, they were anesthetized again by intraperitoneal injection. The anesthesia was satisfied, and then the rat's chest was taken through a median incision to expose the chest cavity and heart. The left atrium was cannulated to the aorta, the catheter position was ligated and fixed, and then, 250 mL of phosphate buffer saline (PBS) solution with a concentration of 0.01 mol/L was quickly perfused into the right atrial appendage. After the liquid became clear, 4% paraformaldehyde was slowly perfused for 1 hour. After the rat was

hardened and fixed, it was cut along the posterior midline approach to expose the lumbar spine, and the spinal cord tissue of the L4-6 segment was taken out for about 5 mm (the integrity of which should be ensured). It was immediately soaked in a 10% neutral formaldehyde solution, fixed for 48h, dehydrated, and then embedded. The wax blocks obtained in the previous step were fixed on the JJQ-P2016 slicer (Wuhan Junjie Electronics Co., LTD., Wuhan, China), and the slices were cut lengthways at 8 μm. 1 piece was taken from every five pieces, and 10 pieces were taken from each spinal cord specimen. The slices were pasted onto the slides and placed in a 45°C constant temperature air-blowing oven to dry. Then, paraffin was removed from the slices with xylene, and it was dewaxed with high-concentration to low-concentration alcohol and washed with distilled water. The slices immersed in distilled water were dyed in the hematoxylin aqueous solution for 10 min. It was rinsed with water for 1h and immersed in distilled water for 5 min. Subsequently, it was dehydrated with 75% alcohol and 90% alcohol for 10 minutes each. Then, it was immersed in an alcohol eosin stain for 2-3 min. At last, it was dehydrated, transparentized, and sealed. The cell bodies of motor neurons in the anterior horn of the spinal cord were counted directly under the microscope (200 ×). The morphological changes of spinal cord tissues were observed in 10 high-power fields from each observation section at 5 different time nodes, and the anterior horn motor neurons were counted. The gray matter of the spinal cord was classified into the anterior and posterior parts by the horizontal line passing through the central canal, and the ventral side of the dividing line was the anterior horn. The presence and distribution of neurons and pathological changes of neurons were generally identified by Nissl bodies. Motor neurons could be distinguished from glial and inflammatory cells by their size, shape, and aggregation of Nissl bodies. A cell with a multipolar body, granular cytoplasm, and nucleoli belonged to a neuron regardless of its size, but those with typical nuclei of astrocytes, oligodendrocytes, and microglia were excluded[10].

Determination of Muscle Wet Weight Maintenance Rate and Muscle Fiber Cross-Sectional Area Recovery rate (RR)

The rats were sacrificed 14 and 28 days after the modeling. The calf gastrocnemius and tibialis anterior muscles of the rats were completely removed, and the surface connective tissue was removed. The blood on the tissue surface was blotted with filter paper, and the tissue was weighed on an electronic analytical balance. Then, it was compared with the wet weight of healthy lateral tibialis anterior muscle and gastrocnemius muscle, and the muscle weight-maintaining rate (MWMR) was calculated[11]. Equation (1) shows the calculation of MWMR.

(1)

$$MWMR = \frac{M_t}{M_C}$$

In Equation (1), M_t represented the muscle weight of the experimental side, and M_C represented that of the control side. The gastrocnemius and tibialis anterior muscle tissues from both the normal and injured sides were immediately placed in 10% formalin solution and fixed for 24h. The muscle was dehydrated by gradient ethanol and embedded in paraffin. Then, it was sectioned with a thickness of 5 microns, stained with HE, re-stained with hematoxylin, dehydrated, transparentized, sealed, and observed. Leica-Qwin image digital analysis software was adopted to randomly select 5 fields at 200 magnifications, measure the number of all muscle cells and the total cross-sectional area in the selected fields, and calculate the average value of the cross-sectional area of each muscle cell. The ratio of the experimental area to the control area was adopted for statistical analysis of the above indicators, and the histopathological indicators of muscle cells were expressed as cross-sectional area recovery rate (CSARR)[12].

Calculation of Axon Passing Rate and Axon Density in Nerve Tissue

The rats were anesthetized on the 21st day after modeling. After the anesthesia was satisfied, the sciatic nerve was exposed through the original incision. The tibial nerve (TN) and common peroneal nerve (CPN) were carefully separated during the surgery, and nerve tissues of the TN and CPN with a length of 3 mm were taken at 5 mm above and below the anastomotic plane. After the tissue was cut, 10% formalin fixative needed to be quickly put into the tissue to achieve the goal of infiltration of fixative into the tissue as soon as possible, thus maintaining the original tissue results. The amount of fixative solution to the volume of tissue block was generally 20:1. The tissue blocks could not be attached to the wall of the container. After the fixed specimens

were sliced according to the steps of washing, dehydration, hardening, transparency, waxing, spreading, and sticking, the Luxol Fast Blue staining was performed to stain and seal the neural tissues[13]. The Image-Pro Plus 6.0 software was adopted to calculate the number of stained axons, and axonal density (AD) was calculated in Equation (2).

(2)

$$r_A = \frac{M}{S}$$

In Equation (2), r_A represents AD, M represents the number of axons; and S represents the area of nerve tissue; Equation (3) shows the calculation of APR.

(3)

$$R_A = \frac{r_r}{r_n}$$

In Equation (3), R_A refers to APR, r_r represents the proximal AD, and r_n refers to the distal AD.

Detection of Immunohistochemistry for the Expression of Bcl-2 and Bax Protein

After the extracted spinal cord tissue of the L4-6 segment was fixed, dehydrated, embedded, and sectioned, the sections were further dewaxed, hydrated, and washed with PBS. At room temperature, the tissue was soaked in 3% hydrogen peroxide for 10 min and washed with sucrose PBS buffer 3 times for 3 min each, and then it was cooled down to room temperature. Then, after rinsing with PBS buffer, 50 μL of anti-Bcl-2 and Bax antibody was added into the primary antibody, and the cells were placed at 37°C for 1h and rinsed with PBS buffer 3 times. 50 μL secondary antibody was dropped, and it was placed at 37°C for 1h and rinsed with PBS buffer 3 times. DAB was adopted for the coloration for 8 min. Then, it was washed with PBS buffer 3 times, with the hematoxylin re-staining for 2 min, hydrochloric acid alcohol differentiation, and tap water washing for 10 min. Subsequently, it was dehydrated, transparentized, and sealed. The expression of Bcl-2 and Bax in tissues was observed under the light microscope. Brown or brown staining of cytoplasm was considered positive cells. The mean optical density of positive cells was determined by the Image-Pro Plus 6.0.

Statistical Analysis

The experimental data were processed and analyzed with SPSS 20.0 statistical software (IBM Corp., Armonk, NY, USA). The measurement data was expressed as mean ± standard deviation ($\overline{x}$ ±s), and count data was expressed in percentage (%). The χ^2 test was applied. $p<0.05$ indicated that the difference was statistically significant.

Results

Analysis on Hematoxylin-Eosin (HE) Staining Results

On the 7th day after modeling, the study observed the neuronal cells in the anterior horn tissue of the spinal cord of three groups of rats using a 200x inverted microscope, as shown in Figure 1. After staining, the spinal anterior horn tissue of the rats in group A showed large and medium-sized neuron cell bodies, showing a star structure, and the neurons were mostly round with large nuclei. After staining, the anterior horn tissue of the spinal cord of rats in group B showed that the nucleus of neuronal cells was dense and darkly stained, and the cytoplasm was stained dark red. The anterior horn tissue of the spinal cord of rats in group C was stained, and the

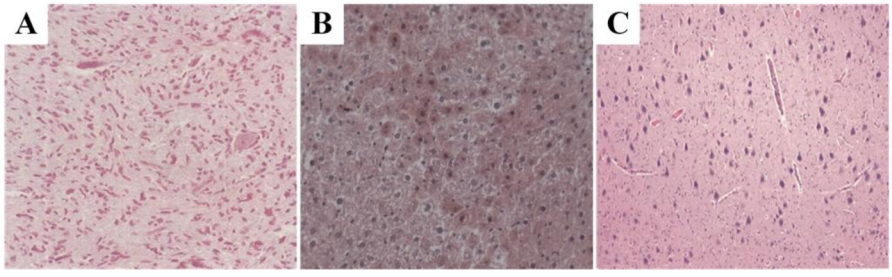

Figure 1. HE staining results of the anterior horn of the spinal cord at the 7th day after modeling. **A-C**, showed the HE staining result of spinal cord anterior horn in group A, B, and C at the 7th day after modeling, respectively (Magnification **A-C**, 40x).

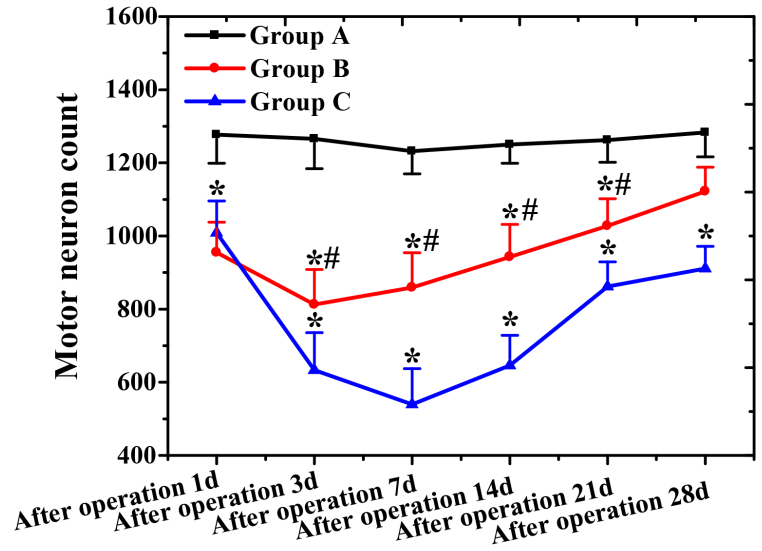

Figure 2. Comparison of neuron counts in different groups at different times. Numbers in horizontal coordinate indicated the days after the surgery (for example, 1 meant the 1st day after the surgery). (*indicated a significant difference in contrast to group A (p<0.05); and # indicated p<0.05 in contrast to group C).

neuron tissue structure was disordered, and the number was visibly smaller.

Count of Motor Neurons

The motor neurons in different time periods after modeling (Figure 2) showed that the number of neurons in group A was in a stable state during the entire observation period. On the 28th day after surgery, the number of neurons in the other two groups decreased before increasing, but remained lower than that in group A. The lowest point was reached on the 7th day after surgery. In contrast to group A, the number of neurons in group B was significantly different on the 1st, 3rd, 7th, 14th, and 21st day after the surgery (p<0.05). On the 28th day after the surgery, the number of neurons in the three groups was not statistically different (p>0.05). Differences between group C and group A on the 1st, 3rd, 7th, 14th, 21st, and 28th day after the surgery were statistically significant (p<0.05); the number of motor neurons in the anterior horn of the spinal cord in group B was higher than that in group C after 3, 7, 14, and 21 days after the surgery (p<0.05).

Comparison of MWMR at Different Times Among Different Groups

MWMR for rats of the three groups were compared and analyzed on the 14th and 28th day after the surgery (Figure 3). It revealed that the MWMR on the 14th day was not statistically different (p>0.05), but that in group B was higher than that in the other two groups on the 28th day (p<0.05), and rats in group B had the lower MWMR than those in group C (p<0.05).

Comparison of CSARR Among Different Groups

The study compared the cross-sectional area of three groups of muscle cells at 28 days after surgery using a 200x inverted microscope (MCCA) and CSARR. In groups B and C, there was an insignificant difference in the muscle fiber area of the experimental side and the healthy side at 28d after surgery. In group A, the muscle fiber area of the experimental side was reduced at different time periods compared with the healthy side (Figure 4A). The CSARR of group B and group C was markedly increased compared with group A, and the CSARR of group B was statistically different from that of group A (p<0.05). The CSARR of group C was evidently different from that of group A (p<0.01), and the CSARR of group B was lower than that of group C (p<0.05) (Figure 4B and 4C).

Analysis and Comparison of APR and AD

The APR and AD of the three groups of rats on the 14th day after the surgery were compared and analyzed (Figures 5 and 6). It disclosed that the proximal AD, distal AD, and APR of group B were lower observably than those of group

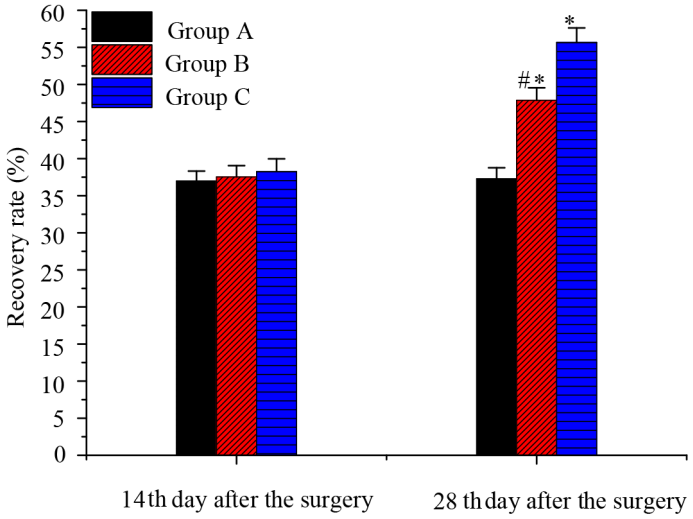

Figure 3. Comparison of recovery rate of muscle wet weight in three groups at different times. (* indicated $p<0.05$ in contrast to group A; and # represented $p<0.05$ in contrast to group C).

A ($p<0.05$), those in group C were extremely different from those in group A ($p<0.01$), and those of group B were higher than those of group C ($p<0.05$). The APR and AD of the three groups of rats were compared on the 28th day after the surgery, and the results were shown in Figure 7 below. The proximal AD, distal AD, and APR of group B were significantly lower than those of group A ($p< 0.05$), and the distal AD and APR of group C were very different from those in group A($p<0.01$), and the proximal AD, distal AD and APR of group B were higher than those of group C ($p<0.05$).

Analysis of the Expression of Bcl-2 and Bax

On the 28th day after surgery, the expression levels of Bcl-2 and Bax in three groups of rats were compared and analyzed under a 200x inverted microscope, as shown in Figure 8 and Figure 9. It suggested that both Bcl-2 and Bax were inside the cytoplasm, and there was no positive staining result for rat tissues in group A. The expression of Bcl-2 and Bax protein in the anterior horn tissue of the spinal cord of rats in groups B and C showed the same trend of first decreasing and then increasing. The expression of Bcl-2 and Bax protein in group B was much higher than that in group C ($p<0.05$).

Discussion

It is generally believed that Wallerian deformation and axonal regeneration will occur once the nerve fibers of the central and peripheral nervous systems are damaged[14,15]. Sciatic nerve injury is the thickest

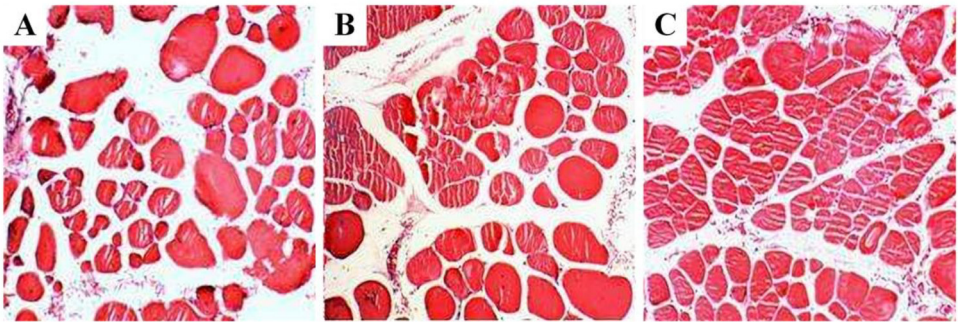

Figure 4. Comparison of cross-sectional area of muscle cells on the 28th day after operation. **A-C**, showed the MCCA at the 28th day after the surgery in groups A-C, respectively. (Magnification A-C, 400x).

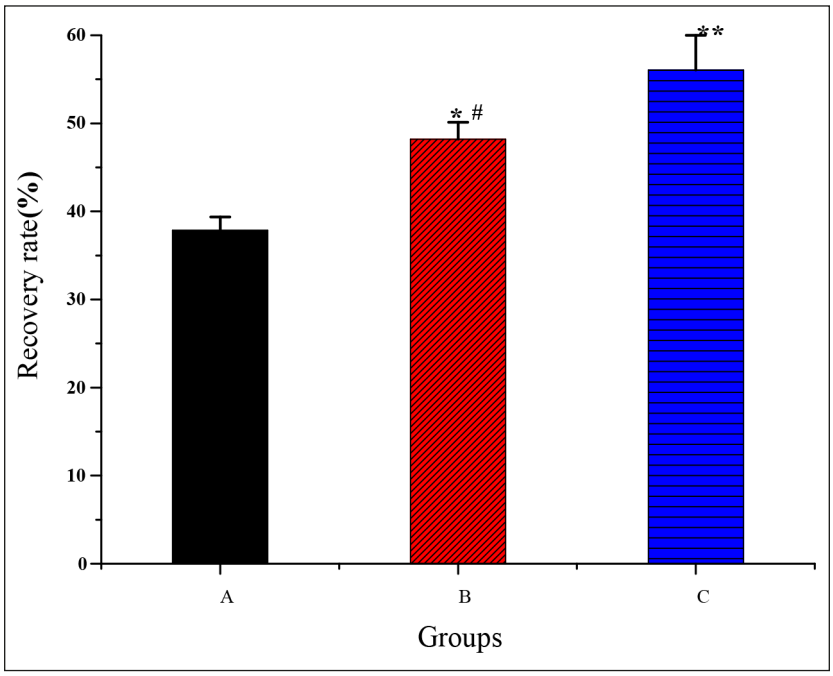

Figure 5. Comparison of recovery rates of three groups of mouse cell cross-sectional areas. (**indicated $p<0.01$ comparing with group A; *suggested $p<0.05$ comparing with group A; and #suggested $p<0.05$ comparing with group A).

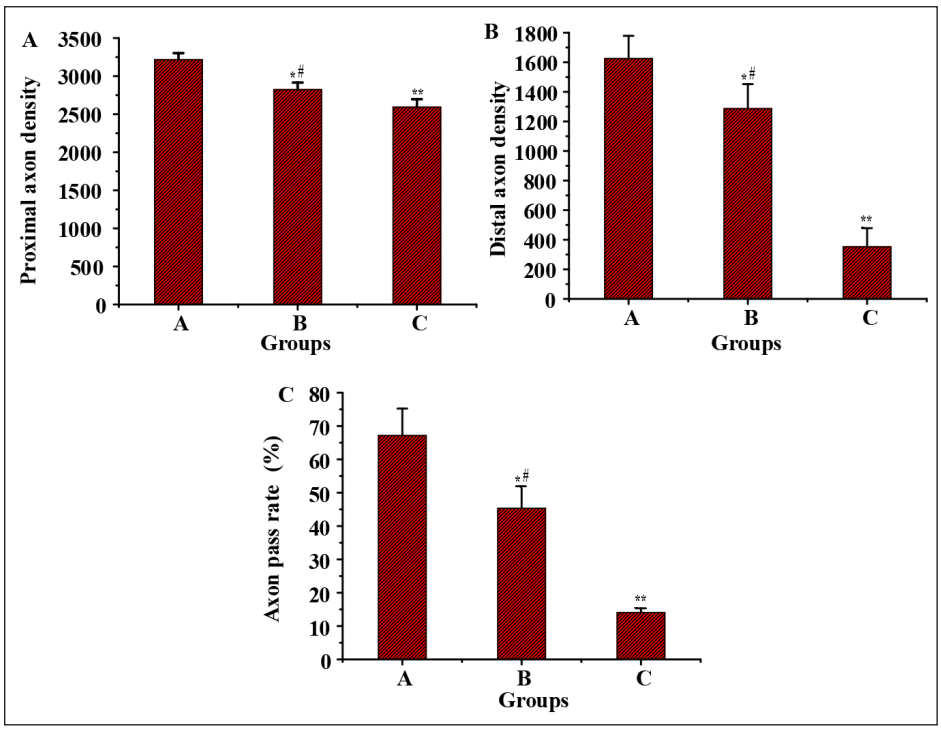

Figure 6. Comparison of axonal density and axonal transit rate on the 14th day after operation in three groups of rats. **A-C**, showed the comparison of proximal AD, distal AD, and APR of the rats at the 14th day after the surgery, respectively). (** indicated $p<0.01$ in contrast to group A; * and # suggested $p<0.05$ comparing with group A and C, respectively).

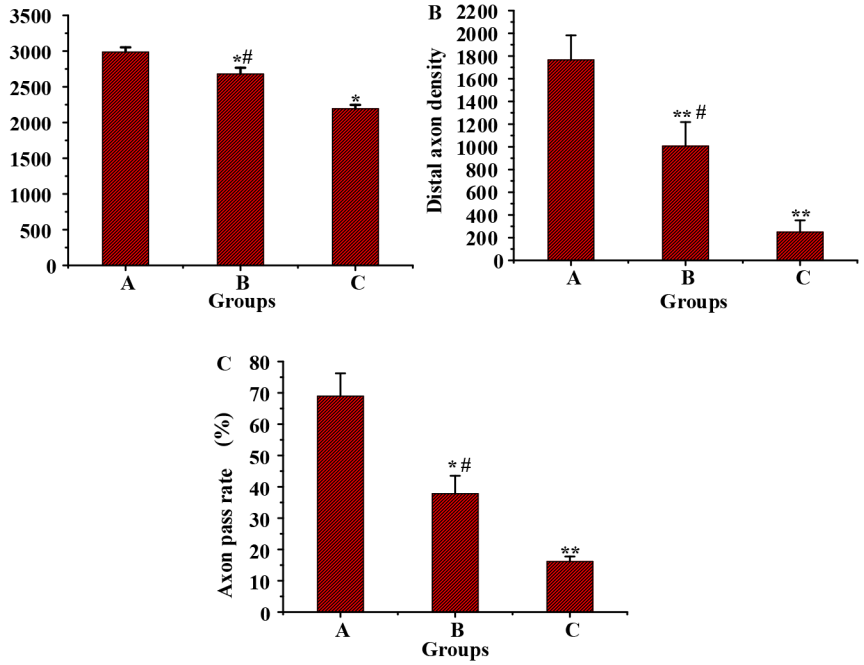

Figure 7. Comparison of axonal density and axonal transit rate of three groups of rats on the 28th day after operation. **A-C**, showed the comparison of proximal AD, distal AD, and APR of the rats at the 28th day after the surgery, respectively). (** indicated $p<0.01$ in contrast to group A; * and # suggested $p<0.05$ comparing with group A and C, respectively).

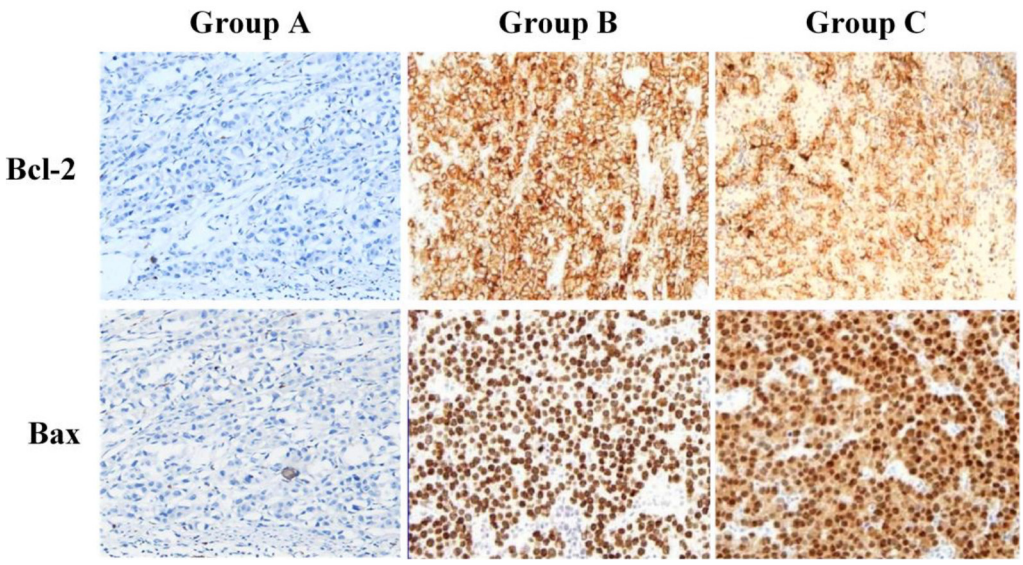

Figure 8. Staining results of Bcl-2 and Bax protein in the spinal anterior horn tissue of rats in different groups (Magnification: 100x).

and most important peripheral nerve in humans and animals. TN and CPN are two significant branches of the sciatic nerve[16]. The effect of functional recovery after peripheral nerve injury mainly depends on the speed and quality of new axon regeneration. Although the peripheral nerve injury is located in the axon, the axon injury is essentially a kind of cell injury, which will inevitably affect the corresponding neuronal cell body. The functional state of neurons will also affect the regeneration and functional recovery of axons[17]. TN and CPN injury models were established through animal models, and the recovery abilities of these two kinds of nerves

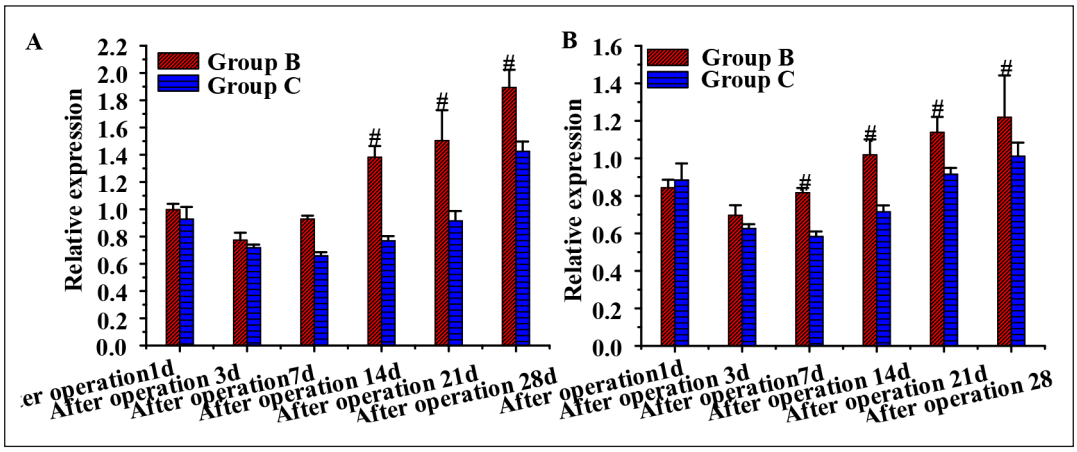

Figure 9. A-B, Comparison on expression of Bcl-2 and Bax protein protein in the spinal anterior horn tissue of rats in different groups. Numbers in horizontal coordinate indicated the days after the surgery (for example, 1 meant the 1st day after the surgery) (# indicated $p<0.05$ to group C).

were compared and analyzed. The experimental results show that TN and CPN have different regeneration speeds and capacities. After 28 days of recovery, the number of neurons had no difference from that of normal rats. The study showed that after peripheral nerve injury, there was no significant change in myelin sheath within 4 days[18]. After 14 days, the distal myelin sheath was decomposed, and nerve regeneration occurred again about 1 month later, which was similar to the situation in this study. Group B and C showed a trend of decreasing first and then increasing, which may be related to the morphological changes and apoptosis of neurons. According to some studies, apoptosis can be observed at the earliest 3 days after peripheral nerve injury, and the number of apoptotic cells is the largest at 7 days, and then, gradually decreases[19]. Some of the regenerated fibers began to pass through the anastomotic stoma, even into the effector, and the neural feedback pathway was partially established. The neurotrophic factors secreted by distal proliferating Schwann cells and a small part of targeted neurotrophic factors are ingested, and they are retrogradely transported to neurons to promote neuronal regeneration, thus increasing the number of neurons[20]. The 28th postoperative study showed that the recovery of TN function was better than that of CPN after the repair of sciatic nerve injury. The results of this study are consistent with those of Cao et al[21]. In this study, the sciatic nerve was repaired by nerve suture. It was found that many axons grew to the distal end of TN[22]. The reason is that the common peroneal nerve is located on the superficial surface, and there are tendons and bone structures nearby. The muscle innervated by the tibial nerve has some innervation. In the process of distal growth, the regenerative ability of the regenerative axons of TN and CPN is different[23].

After peripheral nerve injury, there will be retrograde degeneration of proximal nerve fibers and degeneration or death of proximal neurons to various degrees. This kind of neuronal death is currently considered as neuronal apoptosis[24]. Denaturation and death of neurons will also affect the regeneration and functional recovery of axons, and the whole process is inseparable from the expression of neuron-related genes. The process of apoptosis involves the regulation of a variety of cytokines[25], of which the proto-oncogene Bcl-2 is the most studied and important regulatory factor[26]. It has been found that Bcl-2 can form a heterodimer with Bax protein and block cell apoptosis by inhibiting the activity of caspase-3[27]. The results of this study showed that the expression of Bcl-2 and Bax protein in the spinal cord anterior horn of rats in Group B and Group C showed the same trend of decreasing first and then increasing. It shows that the expression of Bcl-2 and Bax proteins is at the same level after sciatic nerve injury, which is consistent with the research results of Li et al[28]. In addition, the results of this study further found that the expression of Bcl-2 and Bax protein in group B was significantly higher than that in group C, indicating that after TN and CPN were damaged, the probability of death of TN proximal neurons was relatively small. The possible reason is that the functional recovery of the two types of

nerve injuries is different[29]. In addition, research shows that the expression of Bax protein is highly positively correlated with apoptosis[30-32], indicating that the amount of apoptosis in TN is higher than that in CPN in this study. Combined with the number of motor neurons in the anterior horn of the spinal cord and the expression level of Bcl-2 and Bax proteins, TN injury has little effect on the degeneration and death of proximal neurons. This may be the reason why TN function recovers relatively well after TN and CPN are repaired on the same plane.

Conclusions

The difference and molecular mechanism of TN and peroneal nerve recovery ability after the peripheral nerve injury were analyzed based on the rat sciatic nerve injury model. The results showed that the TN had a stronger recovery ability than CPN, and the expression of Bcl-2 and Bax protein of TN was signally higher than that of CPN. However, there are still some deficiencies in this work. That is, only the differences in biology and apoptotic factors are analyzed, but the differences in the corresponding omics level after the two kinds of nerve injury were not analyzed. In the future, the differences in transcriptome and proteomic levels between the two types of nerve injury will be further analyzed. In conclusion, this work provided a reference for the clinical diagnosis and treatment of peripheral nerves.

Conflict of Interest
The authors declare that they have no conflict of interests.

Ethics Approval
All experimental protocols were approved by the Animal Care Committee of Weifang People's Hospital (Ethical code: 20220918012) and followed the Guide for the Care and Use of Laboratory Animals published by the US National Institutes of Health (2011). The study has been conducted in accordance with ARRIVE guidelines.

Data Availability
The dataset used and/or analyzed during the current study are available from the corresponding author on reasonable request.

Authors' contributions
WG, YZ, and JZ designed the experiments and analyzed the experimental results. XJ and WX interpreted data and supervised the experiment, and WG drafted the paper and revised it. All authors read and approved the final manuscript.

Funding
None.

ORCID ID
Jian Zhang: 0000-0002-7762-4570.

References

1) Hewson DW, Bedforth NM, Hardman JG. Peripheral nerve injury arising in anaesthesia practice. Anaesthesia 2018; 73: 51-60.
2) Sullivan R, Dailey T, Duncan K, Abel N, Borlongan CV. Peripheral nerve injury: stem cell therapy and peripheral nerve transfer. Int J Mol Sci 2016; 17: 2101.
3) Huang S, Borgland SL, Zamponi GW. Peripheral nerve injury-induced alterations in VTA neuron firing properties. Mol Brain 2019; 12: 89.
4) Duarte-Moreira RJ, Castro KV, Luz-Santos C, Martins JVP, Sá KN, Baptista AF. Electromyographic biofeedback in motor function recovery after peripheral nerve injury: an integrative review of the literature. Appl Psychophysiol Biofeedback 2018; 43: 247-257.
5) Deshmukh SD, Samet J, Fayad LM, Ahlawat S. Magnetic resonance neurography of traumatic pediatric peripheral nerve injury: beyond birth-related brachial palsy. Pediatr Radiol 2019; 49: 954-964.
6) Navarro X, Geuna S, Grothe C, Haastert-Talini K. Introduction: thematic papers issue on peripheral nerve regeneration and repair. Anat Rec (Hoboken) 2018; 301: 1614-1617.
7) Kim SW, Lee J, Park J, Ji SC, Min CC. Combination of LIM-kinase 2 and Jun amino-terminal kinase inhibitors improves erectile function in a rat model of cavernous nerve injury. Urol 2019; 131: 136-143.
8) Shi Y, Quan R, Li C, Zhang L, Du M, Xu J, Yang Z, Yang D. The study of traditional Chinese medical elongated-needle therapy promoting neurological recovery mechanism after spinal cord injury in rats. Ethnopharmacol 2016; 187: 28-41.
9) Kim BR, Ha DH, Kim JK, Kim YH. Comparison of MR findings of acute traumatic peripheral nerve injury and acute compressive neuropathy in a rat model. PLoS One 2020; 15: e0240911.
10) Li X, Yang W, Xie H, Wang J, Zhang L, Wang Z, Wang L. CNT/Sericin Conductive Nerve Guidance Conduit Promotes Functional Recovery

of Transected Peripheral Nerve Injury in a Rat Model. ACS Appl Mater Interfaces 2020; 12: 36860-36872.

11) Zhang CH, Ma ZZ, Huo BB, Lu YC, Xu JG. Diffusional plasticity induced by electroacupuncture intervention in rat model of peripheral nerve injury. Clin Neurosci 2019; 69: 250-256.

12) Nicolas N, Kobaiter-Maarrawi S, Georges S, Abadjian G, Maarrawi J. Motor Cortex Stimulation Regenerative Effects in Peripheral Nerve Injury: An Experimental Rat Model. World Neurosurg 2018; 114: e800-e808.

13) Gutierrez T, Oliva I, Crystal JD, Hohmann AG. Peripheral nerve injury promotes morphine-seeking behavior in rats during extinction. Exp Neurol 2021; 338: 113601.

14) Reinhold AK, Rittner HL. Barrier function in the peripheral and central nervous system-a review. Pflugers Arch 2017; 469: 123-134.

15) Poli F, Calistri M, Mandara MT, Baroni M. Central nervous system metastasis of an intradural malignant peripheral nerve sheath tumor in a dog. Open Vet J 2019; 9: 49-53.

16) Zantvoort AV, Setz M, Hoogeveen A, Eerten P, Scheltinga N. Chronic lower leg pain: entrapment of common peroneal nerve or tibial nerve. Der Unfallchirurg 2020; 123: 20-24.

17) Atam C, Orhan Z, Toplu G, Serin M, Karaduman ZO, Öztürk A. Comparison of peripheral nerve repair using ethyl-cyanoacrylate and conventional suture technique in a rat sciatic nerve injury model. Acta Orthop Traumatol Turc 2020; 54; 330-336.

18) Lu Y, Li R, Zhu J, Wu Y, Wang J. Fibroblast growth factor 21 facilitates peripheral nerve regeneration through suppressing oxidative damage and autophagic cell death. Cell Mol Med 2019; 23: 497-511.

19) Lin YF, Xie Z, Zhou J, Yin G, Lin HD. Differential gene and protein expression between rat tibial nerve and common peroneal nerve during Wallerian degeneration. Neural Regen Res 2019; 14: 2183-2191.

20) Bao Q, Liu Q, Wang J, Shen Y, Zhang W. Impaired Limb Functional Outcome of Peripheral Nerve Regeneration Is Marked by Incomplete Recovery of Paw Muscle Atrophy and Brain Functional Connectivity in a Rat Forearm Nerve Repair Model. Neural Plast 2021; 2021: 6689476.

21) Cao J, He B, Wang S, Zhou Z, Gao F, Xiao L, Luo X, Wu C, Gong T, Chen W, Wang G. Diffusion tensor imaging of tibial and common peroneal nerves in patients with guillain-barre syndrome: a feasibility study. J MagnReson Imaging 2019; 49: 1356-1364.

22) Shen Y, Ding Z, Ma S, Ding Z, Huang C. SETD7 mediates spinal microgliosis and neuropathic pain in a rat model of peripheral nerve injury. Brain Behav Immun 2019; 82: 382-395.

23) Chato-Astrain J, Philips C, Campos F, Durand-Herrera D, García-García GD, Roosens A, Alaminos M, Campos A, Carriel V. Detergent-based decellularized peripheral nerve allografts: An in vivo preclinical study in the rat sciatic nerve injury model. Tissue Eng Regen Med 2020; 14: 789-806.

24) Korkmaz MF, Parlakpinar H, Erdem MN, Ceylan MF, Kekilli E. The therapeutic efficacy of dexpanthenol on sciatic nerve injury in a rat model. Br J Neurosurg 2020; 34: 397-401.

25) Horteur C, Forli A, Corcella D, Pailhé R, Lateur G, Saragaglia D. Short- and long-term results of common peroneal nerve injuries treated by neurolysis, direct suture or nerve graft. Eur J Orthop Surg Traumatol 2019; 29: 893-898.

26) Kulsoom B, Shamsi TS, Afsar NA, Memon Z, Ahmed N, Hasnain SN. Bax, Bcl-2, and Bax/Bcl-2 as prognostic markers in acute myeloid leukemia: are we ready for Bcl-2-directed therapy. Cancer Manag Res 2018; 10: 403-416.

27) Zhu L, Hao J, Cheng M, Zhang C, Zhang X. Hyperglycemia-induced Bcl-2/Bax-mediated apoptosis of Schwann cells via mTORC1/S6K1 inhibition in diabetic peripheral neuropathy. Exp Cell Res 2018; 367: 186-195.

28) Li Z, Zhang S, Li J, Zeng H, Wang Y, Huang Y. Nerve regeneration in rat peripheral nerve allografts: Evaluation of cold-inducible RNA-binding protein in nerve storage and regeneration. J Comp Neurol 2019; 527: 2885-2895.

29) Jeong JY, Cha HJ, Choi EO, Kim CH, Kim GY, Yoo YH, Hwang HJ, Park HT, Yoon HM, Choi YH. Activation of the Nrf2/HO-1 signaling pathway contributes to the protective effects of baicalein against oxidative stress-induced DNA damage and apoptosis in HEI193 Schwann cells. Int J Med Sci 2019; 16: 145-155.

30) Skała E, Sitarek P, Toma M, Szemraj J, Radek M, Nieborowska-Skorska M, Skorski T, Wysokinska H, Sliwinski T. Inhibition of human glioma cell proliferation by altered Bax/Bcl-2-p53 expression and apoptosis induction by Rhaponticumcarthamoides extracts from transformed and normal roots. J Pharm Pharmacol 2016; 68: 1454-1464.

31) Zuo KJ, Gordon T, Chan KM, Borschel GH. Electrical stimulation to enhance peripheral nerve regeneration: Update in molecular investigations and clinical translation. Exp Neurol 2020; 332: 113397.

32) Singh A, Shiekh P A, Qayoom I, Srivastava E, Kumar A. Evaluation of polymeric aligned NGCs and exosomes in nerve injury models in diabetic peripheral neuropathy condition. European Polymer Journal 2021; 146: 110-126.